Results in Physics 12 (2019) 244–249

Contents lists available at ScienceDirect

Results in Physics

journal homepage: www.elsevier.com/locate/rinp

Combined metal-assisted chemical etching and anisotropic wet etching for anti-reflection inverted pyramidal cavities on dendrite-like textured substrates

Yu-Keng Lin, Yen-Shin Chen, Chun-Hway Hsueh*

Department of Materials Science and Engineering, National Taiwan University, No. 1, Sec. 4, Roosevelt Rd., Taipei 10617, Taiwan

ARTICLE INFO

Keywords:
Metal-assisted chemical etching
Anisotropic wet etching
Textured substrate
Anti-reflection

ABSTRACT

A simple and low-cost method using the combination of metal-assisted chemical etching (MacEtch) and anisotropic wet etching was performed to fabricate anti-reflection inverted pyramidal cavities on dendrite-like textured silicon substrates. To achieve this, a thin Ag film was deposited on an n-type (100) silicon substrate to form agglomerated Ag particles and MacEtch was performed to obtain vertically aligned etching holes on Si substrate. Subsequently, anisotropic wet etching was conducted and the etchant would penetrate the porous structure to form inverted pyramidal cavities on the dendrite-like structure. Using this two-step etching, excellent anti-reflection behavior was obtained for our textured substrates.

Introduction

Textured silicon substrate has attracted much attention since 1980 s due to its appealing properties including excellent mechanical and electronic performances, enhanced light-harvesting, high surface-to-volume ratios, good biocompatibility and surface adjustability which make it a promising candidate for devices in the fields of biomedical and chemical sensors [1–7], chromatography [8], electronics [9–11], optoelectronics [12–14], energy conversion [15–18] and storage [19–21], thermal power conversion [22] and biomimetic superhydrophobicity [23–26], etc. Fabrication of textured silicon substrates can be classified into two categories: (i) dry etching including reactive ion etching (RIE), inductively coupled plasma (ICP)-RIE, reactive ion beam etching (RIBE) and chemical assisted ion beam etching (CAIBE) [27,28], and (ii) wet etching with chemical etchants; e.g., alkaline [29,30] and acidic [31,32] etchants. For anisotropic wet etching of silicon wafers in alkaline solution, {1 1 1} crystal planes with perfectly smooth lateral side-walls could be achieved [33]. Compared to dry etching, wet etching provides a relatively simple and low-cost approach that allows fabrication of different textured silicon structures with the capability of controlling various parameters, such as shape and diameter of porosity, etching length and orientation, and doping type and level [31].

In this work, we reported an approach to fabricate the anti-reflective structures on n-type (100) silicon wafers using two-step wet etching. To achieve this, the silicon substrates were first treated by metal-assisted chemical etching (MacEtch) to obtain vertically aligned etching holes [31,34,35], and sequentially treated in an alkaline solution for anisotropic wet etching to obtain inverted pyramidal cavities on dendrite-like structures. The morphologies of the obtained structures were investigated using scanning electron microscopy (SEM), and the reflectance of the textured substrates was measured using UV–VIS-NIR spectrophotometer.

Materials and methods

Materials

N-type (100)-oriented Czochralski (Cz) Si wafers (phosphorus doped, 2–5 Ω × cm) with a thickness of 500 μm purchased from The Summit-Tech Company were used in this work. Double side polished wafers were cut into 1 × 1 cm^2 pieces for use. Deionized (DI) water (10–15 MΩ × cm) used to prepare aqueous solutions and for rinsing was produced from an Elix® Essential Water Purification System (Millipore). All chemicals used were of analytical grade and were directly used as received without any further purification. Acetone (CH_3COCH_3, 100%) and ethanol (EtOH, C_2H_5OH, 95%) were purchased from UNI-ONWARD Corporation. Sulfuric acid (H_2SO_4, 95.0–97.0%, for analysis, Reag. ISO, Reag. Ph. Eur) and hydrogen peroxide (H_2O_2, 30%, Reag. ISO, Reag. Ph. Eur.) were purchased from Honeywell Fluka™. Ag slug (3 × 6 mm, 99.99%) was purchased from Gredmann. Hydrofluoric acid (HF, 49%) and isopropyl alcohol (IPA,

* Corresponding author.
E-mail address: hsuehc@ntu.edu.tw (C.-H. Hsueh).

https://doi.org/10.1016/j.rinp.2018.11.051
Received 15 November 2018; Accepted 16 November 2018
Available online 27 November 2018

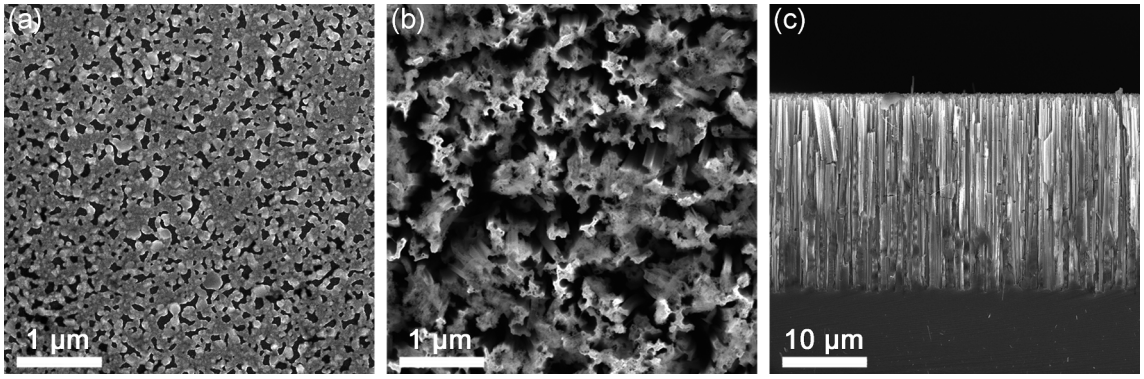

Fig. 1. SEM images showing (a) top-view of agglomerated Ag nanoparticles on Si substrate resulting from deposition of 20 nm-thick Ag film, (b) top-view and (c) side-view of silicon with Ag agglomerates after MacEtch treatment.

$(CH_3)_2CHOH$, 100%) were purchased from Taiwan Maxwave Co. Nitric acid (HNO_3, 65%, Reag. ISO) and Sodium hydroxide (NaOH, ACS Reagent) were purchased, respectively, from PanReac AppliChem and Fisher Scientific.

MacEtch process

The Si substrate was first processed using MacEtch. As-cut silicon was cleaned by ultrasonication with acetone, EtOH and DI water sequentially for 30 min each, immersed in an acidic piranha solution (3:1 mixture of H_2SO_4 and H_2O_2) for 30 min, and thoroughly rinsed with DI water before Ag deposition. To produce island-like Ag agglomerates for MacEtch, 20 nm Ag film was deposited on as-cut silicon using E-beam evaporator under a background pressure of 5×10^{-5} torr. Ag agglomerates would act as a catalyst to catalyze the holes generation underneath from the localized reaction with the oxidant in an acidic solution. Specifically, the substrate with agglomerated Ag was immersed in the etching solution of $HF/H_2O_2/H_2O$ (with the molar ratio defined by $[HF]/([HF] + [H_2O_2]) = 0.904$ and $[H_2O] = 40.1$ M) at ambient temperature for the desired time. After the MacEtch process, Ag was then removed by dipping the etched silicon into the nitric acid solution ($[HNO_3] = 7$ M) for more than 10 min.

Anisotropic wet etching process

After the MacEtch process and removal of Ag, the textured silicon was then treated in an alkaline etching solution containing DI water, NaOH (1.5 wt%) solution, and IPA (6.5 wt%) at 90 °C for desired time [36,37]. The anisotropic etching would lead to the formation of pyramidal structure exposing crystal planes of {1 1 1} on the (100) flat silicon. The nomenclature of the sample in the present study was determined by the etching time of the two etching processes. For example, the sample 10 + 3 was treated in the etching solution containing HF for 10 min in the first-step etching (MacEtch) and sequentially treated in the alkaline solution for 3 min in the second-step etching (anisotropic wet etching). After the second-step etching, both the microstructure and the reflectance of the textured silicon were characterized.

Microstructure and reflectance measurements

The morphologies of Ag and the microstructure of textured silicon were observed using field-emission SEM (Nova Nano SEM 450 and JeoL JSM-7800F Prime). The reflectance spectra recorded from 300 to 1200 nm were measured by UV–VIS-NIR spectrophotometer (JASCO, V-670) equipped with an integrating sphere with 2.0 nm spectral bandwidth.

Results and discussion

Ag-assisted chemical etching

Fig. 1a shows the SEM image of island-like Ag agglomerates formed on the cleaned silicon after Ag film deposition. Fig. 1b shows the top-view SEM image of silicon with Ag agglomerates after 30 min of MacEtch treatment. Porosities were randomly distributed on silicon and the etched silicon was interconnected. From the side-view SEM image of silicon etched for 30 min shown in Fig. 1c, it could be seen that etching holes were vertical to the surface of the silicon substrate with an average depth of ~22.8 μm.

Anisotropic wet etching

The morphologies of silicon after MacEtch treatment and anisotropic wet etching were examined using SEM. Fig. 2a–e shows the top-view SEM images of silicon treated by MacEtch for 30 min and sequentially treated in the alkaline etching solution for 0.5, 1, 2, 3 and 5 min, respectively. The corresponding side-view SEM images are shown in Fig. 2f–j. During anisotropic wet etching, the etchant would penetrate the porous structure to form dendrite-like structure and inverted pyramidal cavities simultaneously because of anisotropic etching of (100)-oriented Si (see Fig. 2a and f). With the increasing etching time, the inverted pyramidal cavities would grow larger, new inverted pyramidal cavities would form and overlap, and the dendrite-like structure would be etched away starting from the top (see Fig. 2b and g). After 2 min of wet etching (see Fig. 2c and h), the dendrite-like structure was almost consumed, pyramidal structure appeared and grew with etching time, and inverted pyramidal cavities became less. After 5 min of wet etching, the dendrite-like structure was totally consumed and the surface of Si was covered by both the pyramidal and inverted pyramidal structure (see Fig. 2e and j).

Based on Fig. 2f–j, the depth of the textured structure as a function of the anisotropic wet etching time is shown in Fig. 3. The depth of the textured structure was determined by the length of the dendrite-like

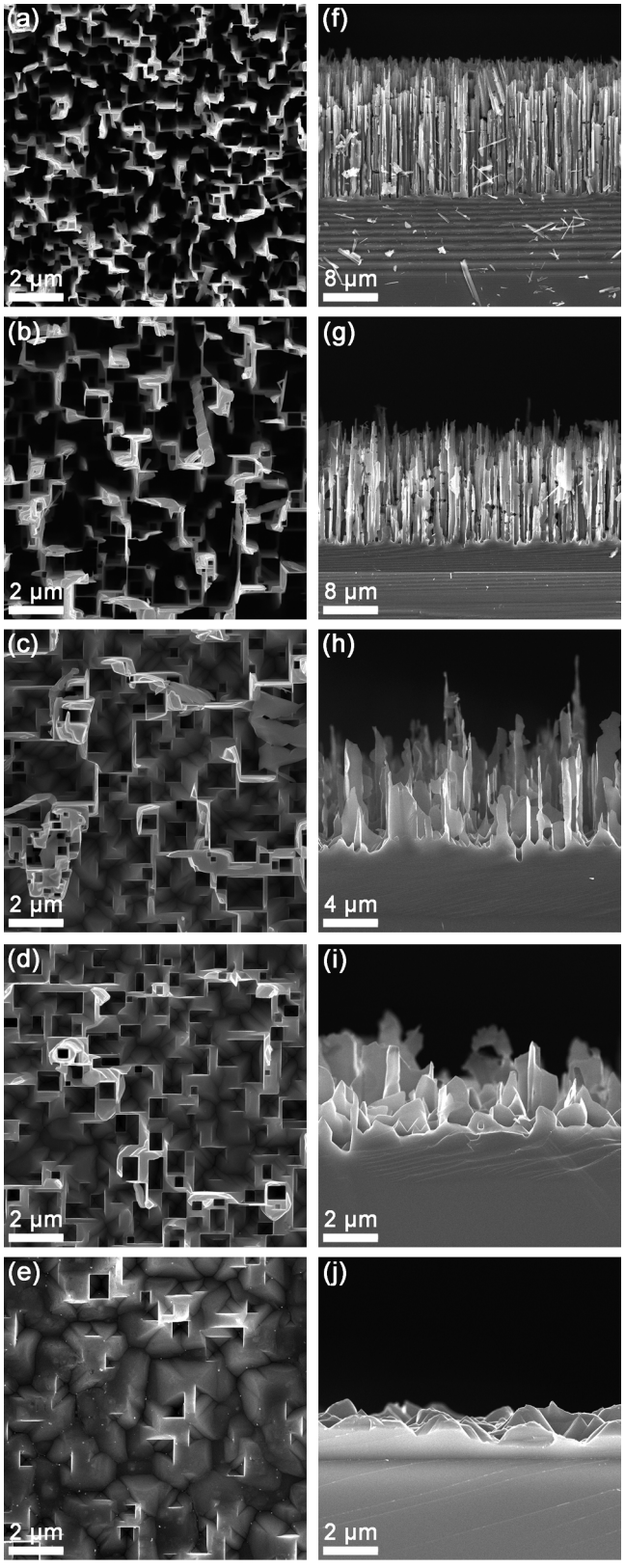

Fig. 2. Top-view SEM images of samples (a) 30 + 0.5, (b) 30 + 1, (c) 30 + 2, (d) 30 + 3 and (e) 30 + 5, and the corresponding side-view SEM images of samples (f) 30 + 0.5, (g) 30 + 1, (h) 30 + 2, (i) 30 + 3 and (j) 30 + 5.

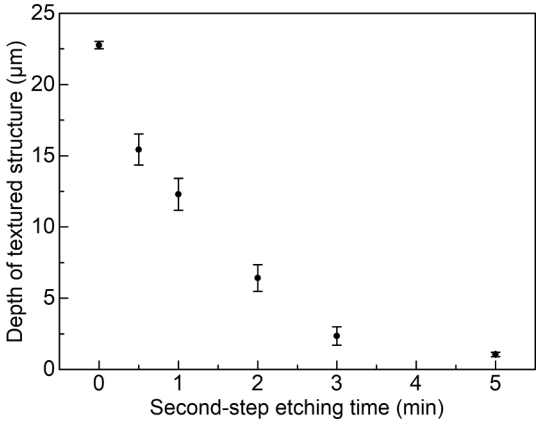

Fig. 3. The depth of the textured structure as a function of anisotropic wet etching time.

structure initially, and the dendrite-like structure was consumed and became shorter with the etching time. The consumption of the dendrite-like structure was accompanied by the appearance and growth of the inverted pyramidal cavities during the anisotropic wet etching process. As the etching depth approached the root of dendrite-like structure, the pyramidal structure started to appear and determined the depth of the textured structure.

The effects of first-step etching; i.e., MacEtch, time were also examined. Fig. 4a–d show the top-view SEM images of silicon treated by MacEtch for 5 min and subsequently treated in the alkaline etching solution for 0.5, 1, 2 and 3 min, respectively. Replacing 5 min by 10 min for MacEtch, the corresponding top-view SEM images of silicon are shown in Fig. 4e–h. While longer MacEtch time would result in deeper etching holes on the substrate, the corresponding textured structures would last longer and the pyramidal structure would appear later in the alkaline etching solution during the second-step etching process.

It is worth noting that MacEtch of Si substrate in a solution containing HF and H_2O_2 followed by anisotropic wet etching in various solutions (e.g., KOH and TMAH) has been performed elsewhere [38,39]. However, anisotropic wet etching was performed at a relatively low temperature (20 °C) previously to separate each Si nanowire from the bunched nanowire obtained from the MacEtch process, and the morphology of the textured substrate was tapered nanowires [38,39]. On the other hand, we applied anisotropic wet etching at a relatively high temperature (90 °C) to enhance the effects of anisotropic etching. As a result, the morphology of our textured substrate was inverted pyramidal cavities on the dendrite-like textured structure that was significantly different from the previous work.

It is also worth noting that the same two-step etching has been performed elsewhere in the reverse order (i.e., anisotropic wet etching followed by MacEtch) [36,40]. However, depending upon the order of the two-step etching process, the morphologies and thus the reflectance spectra would be different. The morphology obtained from previous studies using the same two-step process in the reverse order was the micro-scaled pyramid with nanoporous surface layer textured structure [36,40] and was significantly different from the morphology of our textured substrates. Nevertheless, using MacEtch followed by anisotropic wet etching would consume the MacEtch-generated nanostructures with the increasing anisotropic etching time in our work. On the other hand, using the same two-step procedure performed in the reverse order would reduce surface reflectance instead of consuming the MacEtch-generated nanostructures.

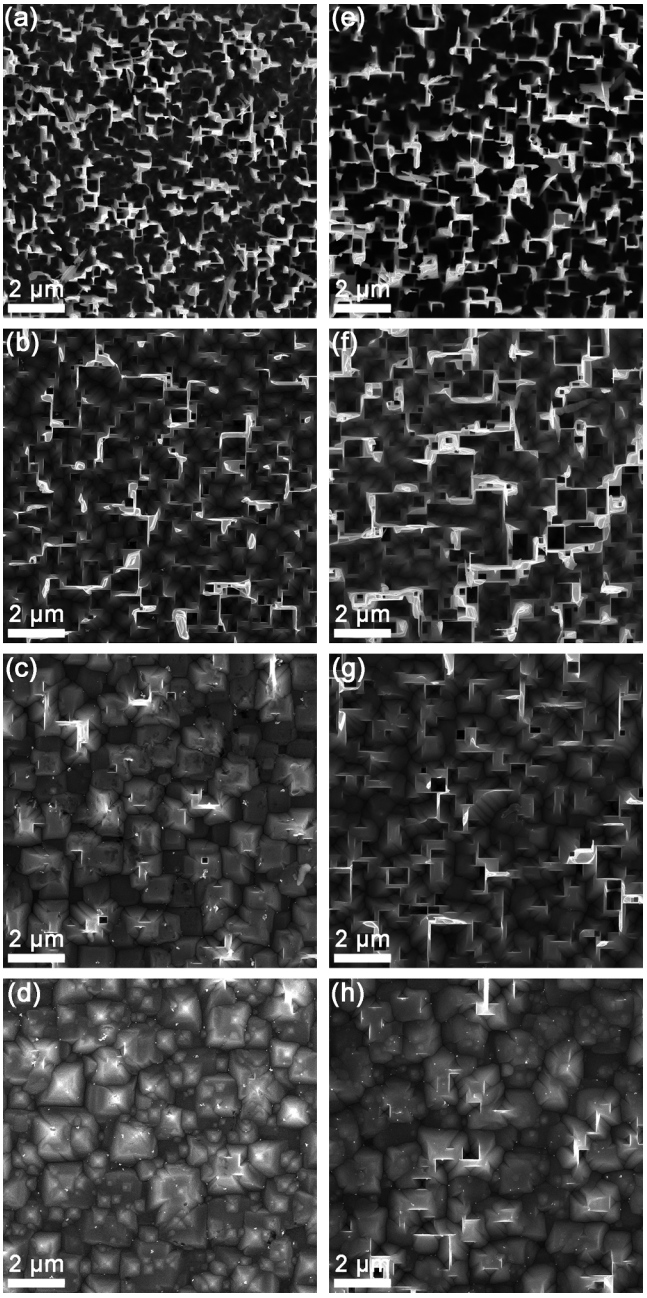

Fig. 4. Top-view SEM images of samples (a) 5 + 0.5, (b) 5 + 1, (c) 5 + 2, (d) 5 + 3, (e) 10 + 0.5, (f) 10 + 1, (g) 10 + 2 and (h) 10 + 3.

Reflectance of textured silicon

The reflectance spectra of the textured substrates in the wavelength range of 300 to 1200 nm were measured using UV–Vis-NIR spectrophotometer and are shown in Fig. 5a–c, respectively, for the MacEtch time of 5, 10 and 30 min at different second-step etching time. In Fig. 5a, the reflectance spectra for samples treated by 5 min of the MacEtch process and then different durations (0, 0.5, 1, 2 and 3 min) of second-step etching were measured. The reflectance of the sample increased in general when the second-step etching was involved, and the second-step etching was not beneficial in reducing the reflectance of the sample. Only the sample 5 + 0.5 exhibited a lower reflectance in the wavelength range of 370 to 527 nm than the sample 5 + 0. Replacing 5 min by 10 min for the MacEtch, the corresponding results of Fig. 5a are shown in Fig. 5b. During the second-step etching, the reflectance at ~500 nm (the peak emission of the sun determined by Wien's law [41]) showed an initial decrease (see sample 10 + 0.5) and it then increased when the second-step etching time increased above 0.5 min. Fig. 5c shows the reflectance spectra of samples treated by MacEtch for 30 min at different durations of second-step etching. In the absence of the second-step etching, the reflectance of the sample 30 + 0 was relatively high compared with samples 5 + 0 and 10 + 0. During the second-step etching, the reflectance at ~500 nm decreased drastically for 0.5 and 1 min of etching time; however, it then displayed a rise as the second-step etching increased above 1 min. Overall, the sample 30 + 1 exhibited the lowest reflectance in the wavelength range of 362–571 nm among all samples in this work.

To examine the general trend of the dependence of reflectance on the first- and the second-step etching time, the reflectance at the wavelength 500 nm for the samples studied in Fig. 5a–c is shown in Fig. 5d. It is worth noting that the samples 5 + 0.5, 10 + 0.5, 30 + 0.5 and 30 + 1 containing both the micro-scaled dendrite-like structure and nano to micro-scaled inverted pyramidal cavities had relatively low reflectance at this wavelength. With prolonged second-step etching time, the dendrite-like structure would be largely consumed and thus the reflectance increased monotonically. Also, although the presence of micro-scaled inverted pyramidal cavities could reduce the reflectance in the spectral range near the peak emission of the sun of 500 nm as shown in Fig. 5d, it is not beneficial outside this spectral range as shown in Fig. 5a–c. Hence, depending on the intended application, judicial choice of etching treatments of the substrate should be made.

Conclusions

To summarize, fabrication of effective anti-reflection textured silicon substrates by the combination of MacEtch and anisotropic wet etching was presented in this study. This technique is a relatively low-cost and simple silicon etching method which is capable of making structures at the wafer scale. By applying this combined etching technique, a textured structure of nano to micro-scaled inverted pyramidal cavities on the micro-scaled dendrite-like structure was obtained. This unique texture resulted from the porous structure fabricated using MacEtch which provided channels for the alkaline etchant to react with the inner part of the structure during anisotropic wet etching to form inverted pyramidal cavities. In our work, the effect of light-harvesting in the wavelength near the peak emission of the sun was the best when the MacEtch time was 30 min and the anisotropic wet etching time was 1 min. The advantages of this substrate such as low cost, enhanced light-harvesting, adjustability and large surface area make it a promising candidate for further use in the fields of sensors, surface-enhanced Raman scattering substrates, solar cells and energy storage.

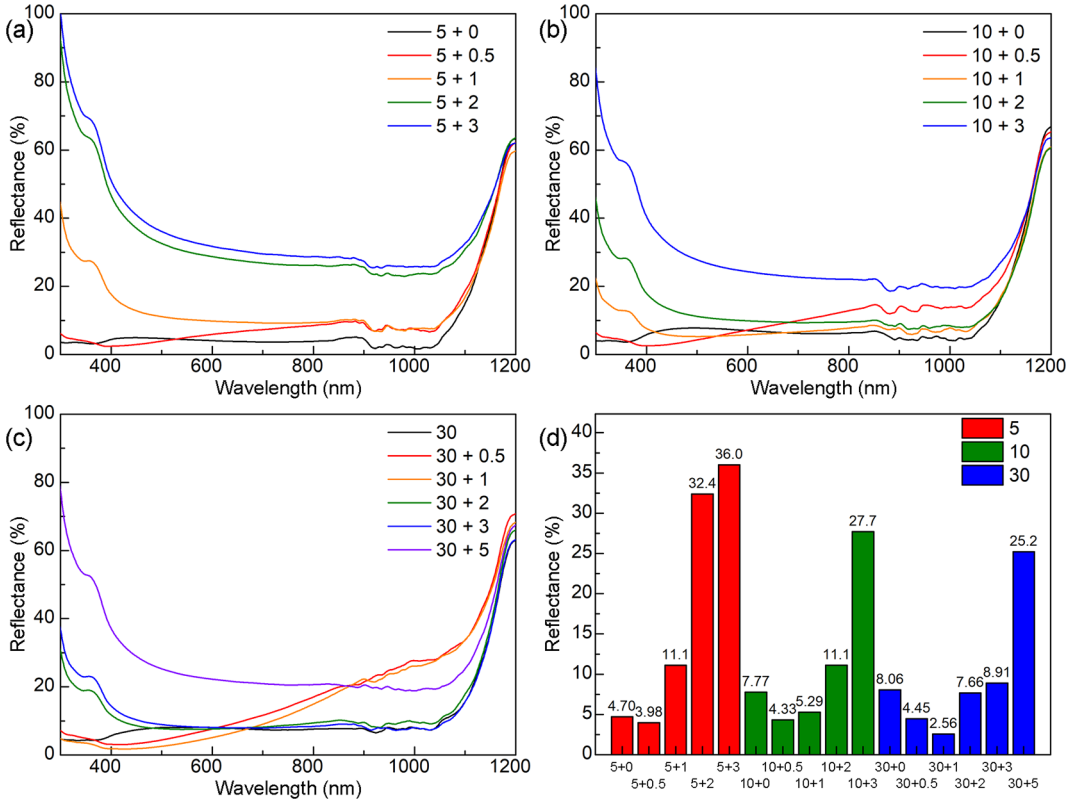

Fig. 5. Reflectance spectra from 300 to 1200 nm for n-type (100) silicon substrates treated by the MacEtch process for (a) 5, (b) 10, and (c) 30 min, and subsequently treated in the alkaline etching solution for different durations. (d) The reflectance at 500 nm for the samples mentioned above.

Declarations of interest

None.

Acknowledgments

The work was supported by the Ministry of Science and Technology, Taiwan under Contract No. MOST 107-2221-E-002-013. A portion of experiments in this work was performed at the National Taiwan University NEMS Research Center and is gratefully acknowledged.

References

[1] He Y, Fan C, Lee ST. Silicon nanostructures for bioapplications. Nano Today 2010;5:282–95. https://doi.org/10.1016/j.nantod.2010.06.008.
[2] Lin VSY, Motesharei K, Dancil KPS, Sailor MJ, Ghadiri MR. A porous silicon-based optical interferometric biosensor. Science 1997;278:840–3. https://doi.org/10.1126/science.278.5339.840.
[3] Cui Y, Wei Q, Park H, Lieber CM. Nanowire nanosensors for highly sensitive and selective detection of biological and chemical species. Science 2001;293:1289–92. https://doi.org/10.1126/science.1062711.
[4] Patolsky F, Zheng G, Lieber CM. Fabrication of silicon nanowire devices for ultra-sensitive, label-free, real-time detection of biological and chemical species. Nat Protoc 2006;1:1711–24. https://doi.org/10.1038/nprot.2006.227.
[5] Huang XJ, Choi YK. Chemical sensors based on nanostructured materials. Sens Actuators B 2007;122:659–71. https://doi.org/10.1016/j.snb.2006.06.022.
[6] Xu J, Kvasnička P, Idso M, Jordan RW, Gong H, Homola J, et al. Understanding the effects of dielectric medium, substrate, and depth on electric fields and SERS of quasi-3D plasmonic nanostructures. Opt Express 2011;19:20493–505. https://doi.org/10.1364/OE.19.020493.
[7] Xu J, Zhang L, Gong H, Homola Jí, Yu Q. Tailoring plasmonic nanostructures for optimal SERS sensing of small molecules and large microorganisms. Small 2011;7:371–6. https://doi.org/10.1002/smll.201001673.
[8] Kirchner TB, Hatab NA, Lavrik NV, Sepaniak MJ. Highly ordered silicon pillar arrays as platforms for planar chromatography. Anal Chem 2013;85:11802–8. https://doi.org/10.1021/ac402261p.
[9] Goldberger J, Hochbaum AI, Fan R, Yang P. Silicon vertically integrated nanowire field effect transistors. Nano Lett 2006;6:973–7. https://doi.org/10.1021/nl060166j.
[10] Schmidt V, Riel H, Senz S, Karg S, Riess W, Gösele U. Realization of a silicon nanowire vertical surround-gate field-effect transistor. Small 2006;2:85–8. https://doi.org/10.1002/smll.200500181.
[11] Himpsel F, McChesney J, Crain J, Kirakosian A, Perez-Dieste V, Abbott NL, et al. Stepped silicon surfaces as templates for one-dimensional nanostructures. J Phys Chem B 2004;108:14484–90. https://doi.org/10.1021/jp049209f.
[12] Canham LT. Silicon quantum wire array fabrication by electrochemical and chemical dissolution of wafers. Appl Phys Lett 1990;57:1046–8. https://doi.org/10.1063/1.103561.
[13] Brus L. Luminescence of silicon materials: chains, sheets, nanocrystals, nanowires, microcrystals, and porous silicon. J Phys Chem 1994;98:3575–81. https://doi.org/10.1021/j100065a007.
[14] Tian B, Zheng X, Kempa TJ, Fang Y, Yu N, Yu G, et al. Coaxial silicon nanowires as solar cells and nanoelectronic power sources. Nature 2007;449:885–90. https://doi.org/10.1038/nature06181.
[15] Garnett E, Yang P. Light trapping in silicon nanowire solar cells. Nano Lett 2010;10:1082–7. https://doi.org/10.1021/nl100161z.
[16] Fan G, Zhu H, Wang K, Wei J, Li X, Shu Q, et al. Graphene/silicon nanowire Schottky junction for enhanced light harvesting. ACS Appl Mater Interfaces 2011;3:721–5. https://doi.org/10.1021/am1010354.
[17] Garnett EC, Yang P. Silicon nanowire radial p−n junction solar cells. J Am Chem Soc 2008;130:9224–5. https://doi.org/10.1021/ja8032907.
[18] Stelzner T, Pietsch M, Andrä G, Falk F, Ose E, Christiansen S. Silicon nanowire-based solar cells. Nanotechnology 2008;19:295203. https://doi.org/10.1088/0957-4484/19/29/295203.
[19] Chan CK, Peng H, Liu G, McIlwrath K, Zhang XF, Huggins RA, et al. High-performance lithium battery anodes using silicon nanowires. Nat Nanotech 2008;3:31–5. https://doi.org/10.1142/9789814317665_0026.
[20] Peng K, Jie J, Zhang W, Lee ST. Silicon nanowires for rechargeable lithium-ion battery anodes. Appl Phys Lett 2008;93:033105. https://doi.org/10.1063/1.2929373.
[21] McSweeney W, Geaney H, O'Dwyer C. Metal-assisted chemical etching of silicon and the behavior of nanoscale silicon materials as Li-ion battery anodes. Nano Res 2015;8:1395–442. https://doi.org/10.1007/s12274-014-0659-9.
[22] Hochbaum AI, Chen R, Delgado RD, Liang W, Garnett EC, Najarian M, et al. Enhanced thermoelectric performance of rough silicon nanowires. Nature 2008;451:163–8. https://doi.org/10.1038/nature06381.
[23] Guo Z, Liu W, Su BL. Superhydrophobic surfaces: from natural to biomimetic to functional. J Colloid Interface Sci 2011;353:335–55. https://doi.org/10.1063/1.2929373.
[24] Cao M, Song X, Zhai J, Wang J, Wang Y. Fabrication of highly antireflective silicon surfaces with superhydrophobicity. J Phys Chem B 2006;110:13072–5. https://doi.org/10.1021/jp061373a.
[25] Shi F, Song Y, Niu J, Xia X, Wang Z, Zhang X. Facile method to fabricate a large-

scale superhydrophobic surface by galvanic cell reaction. Chem Mater 2006;18:1365–8. https://doi.org/10.1021/cm052502n.
[26] Xiu Y, Zhu L, Hess DW, Wong C. Hierarchical silicon etched structures for controlled hydrophobicity/superhydrophobicity. Nano Lett 2007;7:3388–93. https://doi.org/10.1021/nl0717457.
[27] Abe H, Yoneda M, Fujiwara N. Developments of plasma etching technology for fabricating semiconductor devices. Jpn J Appl Phys 2008;47:1435–55. https://doi.org/10.1143/JJAP.47.1435.
[28] Nojiri K. Dry etching technology for semiconductors. Springer; 2016.
[29] Singh PK, Kumar R, Lal M, Singh S, Das B. Effectiveness of anisotropic etching of silicon in aqueous alkaline solutions. Sol Energy Mater Sol Cells 2001;70:103–13. https://doi.org/10.1016/S0927-0248(00)00414-1.
[30] Xi Z, Yang D, Dan W, Jun C, Li X, Que D. Investigation of texturization for monocrystalline silicon solar cells with different kinds of alkaline. Renew Energy 2004;29:2101–7. https://doi.org/10.1016/j.renene.2004.03.003.
[31] Huang Z, Geyer N, Werner P, De Boor J, Gösele U. Metal-assisted chemical etching of silicon: a review. Adv Mater 2011;23:285–308. https://doi.org/10.1002/adma.201001784.
[32] Li X, Bohn P. Metal-assisted chemical etching in HF/H_2O_2 produces porous silicon. Appl Phys Lett 2000;77:2572–4. https://doi.org/10.1063/1.1319191.
[33] Seidel H, Csepregi L, Heuberger A, Baumgärtel H. Anisotropic etching of crystalline silicon in alkaline solutions I. Orientation dependence and behavior of passivation layers. J Electrochem Soc 1990;137:3612–26. https://doi.org/10.1149/1.2086277.
[34] Nien LW, Chien MH, Chao BK, Chen MJ, Li JH, Hsueh CH. 3D nanostructures of silver nanoparticle-decorated suspended graphene for SERS detection. J Phys Chem Lett 2016;120:3448–57. https://doi.org/10.1021/acs.jpcc.5b11940.
[35] Toor F, Miller JB, Davidson LM, Nichols L, Duan W, Jura MP, et al. Nanostructured silicon via metal assisted catalyzed etch (MACE): chemistry fundamentals and pattern engineering. Nanotechnology 2016;27:412003. https://doi.org/10.1088/0957-4484/27/41/412003.
[36] Geng X, Qi Z, Li M, Duan BK, Zhao L, Bohn PW. Fabrication of antireflective layers on silicon using metal-assisted chemical etching with in situ deposition of silver nanoparticle catalysts. Sol Energy Mater Sol Cells 2012;103:98–107. https://doi.org/10.1016/j.solmat.2012.04.020.
[37] Chao BK, Cheng HH, Nien LW, Chen MJ, Nagao T, Li JH, et al. Anti-reflection textured structures by wet etching and island lithography for surface-enhanced Raman spectroscopy. Appl Surf Sci 2015;357:615–21. https://doi.org/10.1016/j.apsusc.2015.09.047.
[38] Jung JY, Guo Z, Jee SW, Um HD, Park KT, Lee JH. A strong antireflective solar cell prepared by tapering silicon nanowires. Opt Express 2010;18:A286–92. https://doi.org/10.1364/OE.18.00A286.
[39] Jung JY, Guo Z, Jee SW, Um HD, Park KT, Hyun MS, et al. A wafer scale Si wire solar cell using radial and bulk p–n junctions. Nanotechnology 2010;21:445303. https://doi.org/10.1088/0957-4484/21/44/445303.
[40] Qi D, Lu N, Xu H, Yang B, Huang C, Xu M, et al. Simple approach to wafer-scale self-cleaning antireflective silicon surfaces. Langmuir 2009;25:7769–72. https://doi.org/10.1021/la9013009.
[41] Walker J, Resnick R, Halliday D. Fundamentals of physics. Wiley; 2008.